Asian Journal of Chemistry; Vol. 38, No. 1 (2026), 209-214
ASIAN JOURNAL OF CHEMISTRY
https://doi.org/10.14233/ajchem.2026.34774

Synthesis of $BaTiO_3$/Graphene Oxide/Polyvinylidene Fluoride Nanocomposite Film based Nanogenerator for Energy Harvesting Application

YADAGIRI RAO YASALA[1], H. MALLESHA[1], KAMMARI SURESH CHARY[2] and Y. PRASHANTHI[1,*]

[1]Department of Chemistry, Mahatma Gandhi University, Nalgonda-508001, India
[2]Naval Material Research Laboratory, DRDO, Shil-Badlapur, Ambernath East, Thane District-421506, India

*Corresponding author: E-mail: prashanthimgu1@gmail.com

Received: 27 August 2025 *Accepted*: 12 December 2025 *Published online*: 31 December 2025 AJC-22240

Piezoelectric based flexible sensors are very important in the field of the wearable electronics and self-powered sensor applications. Herein, the synthesis of barium titanate nanoparticles (BT NPs) with a diameter are in the range of approximately 70-200 nm *via* hydrothermal process is reported. The synthesized BT NPs and graphene oxide (GO) are dispersed in PVDF polymer matrix to fabricate the nanocomposite film. Flexible nanogenerator was developed using BT/GO/PVDF nanocomposite film and copper electrodes and packed in the epoxy polymer. Nanogenerator exhibited the output voltage ~11 V and ~0.34 μW power under repeated mechanical tapping. The robustness of developed nanogenerator was studied under 1000 cycle of continuous mechanical tapping.

Keywords: Barium titanate, Graphene oxide, Hydrothermal, Nanogenerator, Nanocomposite, Epoxy resin.

INTRODUCTION

Energy plays a major role in mankind progress. Fossil fuels-based energy is harnessed and being used in making human life easier. However, most of these come from non-renewable sources and concentrated in a few places and require humongous machines to harvest. This led to the development of methods in tapping renewable energy from solar, wind, tidal, *etc.* sources. Scientific and technological advances are made in extracting energy from these sources. Power generation is generally massive with fossil fuels and these are not spread evenly on the globe and with negative side of environmental pollution [1,2]. On the other hand, renewable energy [3-6] is present in all corners of the world, yet harnessing power from these sources is still a technical challenge. Remarkable progress is made in recent times and extensive research enabled in realizing power from these sources to run many applications like domestic power consumption to small and medium sized electronic devices.

Nevertheless, all these non-renewable and renewable energies are extracted in modest to large scale. So, tapping power from small-scale sources plays a vital role in sustainable energy ecosystem. Small-scale energy sources like piezoelectricity, triboelectricity and pyroelectricity based polymer composite nanogenerator devices PENG [7,8], TENG [9] and PyENG [10] are fabricated to harness power from very simple daily activities. These devices are small and can be utilized for making self-powered wearable electronic devices, technical instruments and remote operated electronics. Flexible and highly efficient nan-generators play important role in the development of new kind of advanced electronics devices in the field of health, power, miniaturized instruments in space and defence applications [11-14].

Polyvinylidene fluoride (PVDF) [15] is one of the most used piezoelectric polymers in field of flexible sensors and actuators due its high energy conversion efficiency approximately 22%. Nevertheless, PVDF is highly flexible, durable, light weight and even it withstands high stress deformation like stretching, bending and twisting. PVDF is available in four crystalline forms (α, β, γ and δ phases) depending upon the processing method. Among these phases β-crystalline phase is most popular form of electroactive phase, which shows piezoelectric behaviour, whereas γ-phase also exhibits piezoelectric along with β-phase due to non-centrosymmetric in nature. For enhancement of fraction of electroactive phases, incorporation of nanofillers like ZnO [16], ceramics ($BaTiO_3$

[17], PZT [18], KNN [19,20]) and graphene oxide (GO) in PVDF matrix is reported. Study of incorporation of nanofillers $BaTiO_3$ and GO were not studies well.

In this work, we report synthesis of $BaTiO_3$ nanoparticles (BT NP) by hydrothermal process. The phase formation and microstructure of BT nanoparticles have been studied. There after nanocomposite film was fabricated by simple casting technique using BT NPs and GO as fillers in the PVDF matrix. This BT/GO/PVDF nanocomposite film is used for the fabrication of nanogenerators through cost effective and simple method. The composite film was used further for fabrication of nanogenerator (NG). The performance of the developed nanogenerator was tested under periodic external mechanical deformation by recurrent tapping using sewing machine. The NG demonstrated an open circuit voltage of approximately 10.5 V (peak-to-peak) and a maximum current of about 0.4 μA under a load of 4.7 MΩ. A highly stable and consistent piezoelectric output signal was observed during repeated vibration cycles, with no mechanical damage evident even after 1000 cycles of mechanical tapping. Performance degradation was minimal, approximately 1-2%. The developed NG is highly robust, efficient, cost-effective and scalable, making it particularly suitable for the development of self-powered, flexible sensor applications [21-25].

EXPERIMENTAL

Synthesis of $BaTiO_3$ (BT) nanoparticle: BT nanoparticles was synthesized by hydrothermal synthesis as reported by Chary *et al.* [21]. Barium acetate 99% pure (Alfa Aesar), titaniumisobutaoxide (Alfa Aesar), acetylacetone AR grade (SRL) and acetic acid AR grade (SRL) were used as the precursor materials for preparing the BT nanoparticles. In this method, titaniumisobutoxide was modified by reacting with pure acetylacetone in 1:2 molar ratio, respectively to control the hydrolysis and condensation reactions of titaniumisobutoxide. A stoichiometric molar ratio of 1 mol of barium acetate dissolved in acetic acid and 1 mol of modified titaniumisobutoxide was magnetically stirred at 50-60 ºC for 8 h, resulting in the formation of a clear deep-yellow solution. Finally, the suspension was transferred into a 100 mL Teflon vessel and further added 30 mL isopropyl alcohol to fill 80% of total volume of the vessel. Total setup was placed in to a Teflon-lined stainless steel tank autoclave. This autoclave was further kept inside an oven at 200 ºC for 10 h. After cooling, grey-coloured fine precipitation was obtained and it was washed thrice by deionized water and once by ethanol at 5000 rpm for 10 min in centrifuge to remove dissolved impurity. The as-obtained powder then was dried in oven at 80 ºC for 10 h.

Preparation of BT/GO/PVDF nanocomposite film: BT nanoparticles (2 wt.%) were dispersed in methylethylketone (MEK) using ultrasonicator for 1 h, there after the suspension was stirred on magnetic stirred for 4-5 h using BYK-20 as surfactant (0.05 wt.% to powder). In other beaker, PVDF powder was dissolved in MEK at 60 ºC for and stirred with magnetic for overnight. The 0.1 wt.% of GO (Sigma-Aldrich) was dispersed in separate beaker using ultrasonicator, thereafter stirred overnight. The prepared suspensions mixed together and stirred for 4-5 h for uniform dispersion in PVDF polymer matrix to form composite solution. The composite solution was casted on Teflon mould, which was cleaned thoroughly with isopropyl alcohol and deionized water then dried. After casting the film was cured at 120 ºC for 8-10 h to get a unform and thin (100 μm) BT/GO/PVDF composite film.

Fabrication of nanogenerator: The developed BT/GO/PVDF composite films was cut into small films like, dimensions of 20 mm (W) × 20 mm (L) × 0.1 mm (T) and a thin gold electrode film was coated using sputtering to reduced contact resistance. This composite film was attached copper electrodes subsequently and packed into the pre-cured epoxy polymer.

Characterization: The structure analysis of the BT nanopowder and BT/GO/PVDF nanocomposite was carried out through powder X-ray diffractometer (Bruker D8 Advance) with Cu*K*α radiation (λ = 1.542 Å) with scanning angle (2θ of 20-60º). The morphology of BT NPs, pure PVDF and BT/GO/PVDF composite films was analyzed by field emission-scanning electron microscope (FE-SEM, Model: Zeiss Supra 40VP, Germany) and transmission electron microscope (HR-TEM). Infrared spectroscopy analysis of Fourier transform infrared (FT-IR) spectroscopy (Thermo electron corporation Nicolet 6700) of PVDF and BT/GO/PVDF composite film was carried out to know bonding nature and formation of electroactive phases in the developed films. The performance of nanogenerator was investigated by recording the output voltage using Oscilloscope (Model: Tektronix TDS 3054C).

RESULTS AND DISCUSSION

XRD studies: X-ray diffraction pattern of BT nanoparticles indicates the formation of single-phase perovskite structure without any secondary phase (Fig. 1a). The broad peaks represent crystallite size is small *i.e.* in the range nano. The broad peak at 45º reveals that combination of [002] and [020] planes, means that formed particles is tetragonal in nature. Due to *c*/*a* ratios is very close to 1, the peaks were merged together. XRD pattern of the PVDF/GO/BT NP nanocomposite films shows the both peaks of PVDF and BT NPs reveals the BT particles are well dispersed in the PVDF matrix, which also support the SEM image. XRD peaks at 18.5º and 20.1º is corresponds to α-phase and β-phase of pure PVDF [21,22] and BT/GO/PVDF composite films as shown in Fig. 1b. XRD reveals, importing the nanofillers in the PVDF matrix, fraction of β-phase increases compared to pure PVDF polymer as shown in Fig. 1b.

Morphological studies: SEM analysis of synthesized BT nanoparticles and PVDF film, BT/GO/PVDF composite films was analyzed by FE-SEM to reveal the morphology and dispersion of BT and GO nanoparticles in the PVDF matrix. The SEM micrograph (Fig. 2) of BT particles indicates the particle are uniform and size is in the range 100-200 nm.

Fig. 2b-c are the SEM micrographs of pure and composite films. The SEM image reveals that the BT and GO fillers are well dispersed in the PVDF polymer matrix depicted in the Fig. 2c.

The BT NP was further analyzed by transmission microscope Fig. 3a, it reveals some particles are in the nano range

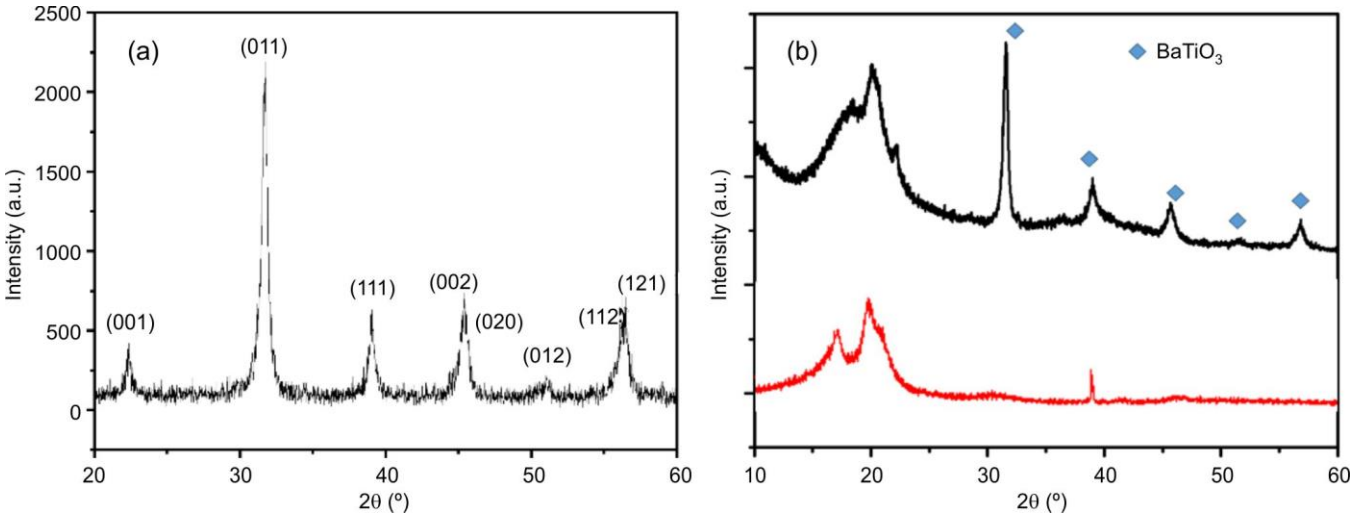

Fig. 1. XRD patterns of (a) BT nanoparticles and (b) pure PVDF and composite film

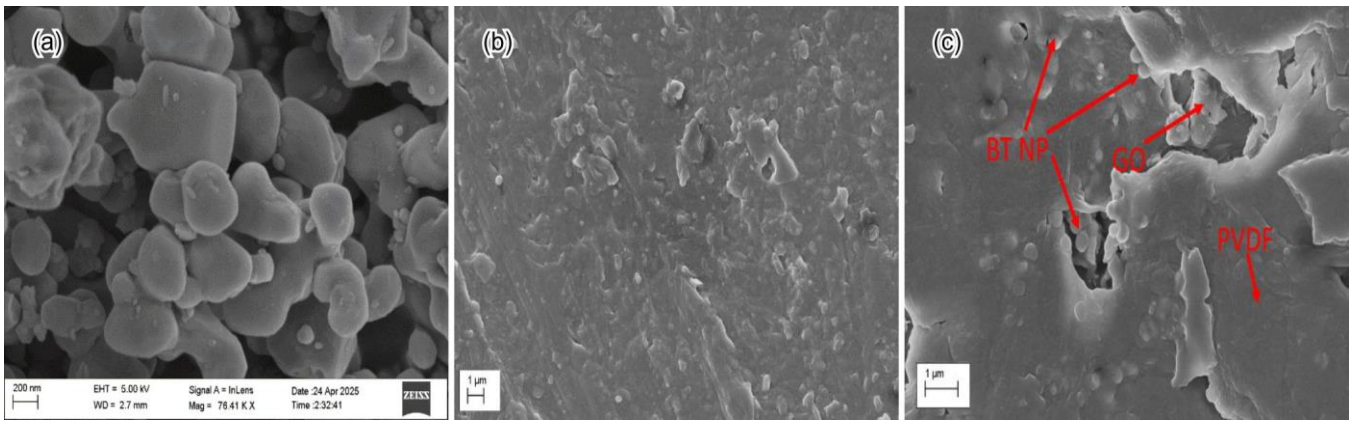

Fig. 2. SEM of (a) BT nanoparticles, (b) PVDF composite film and (c) BT/GO/PVDF composite film

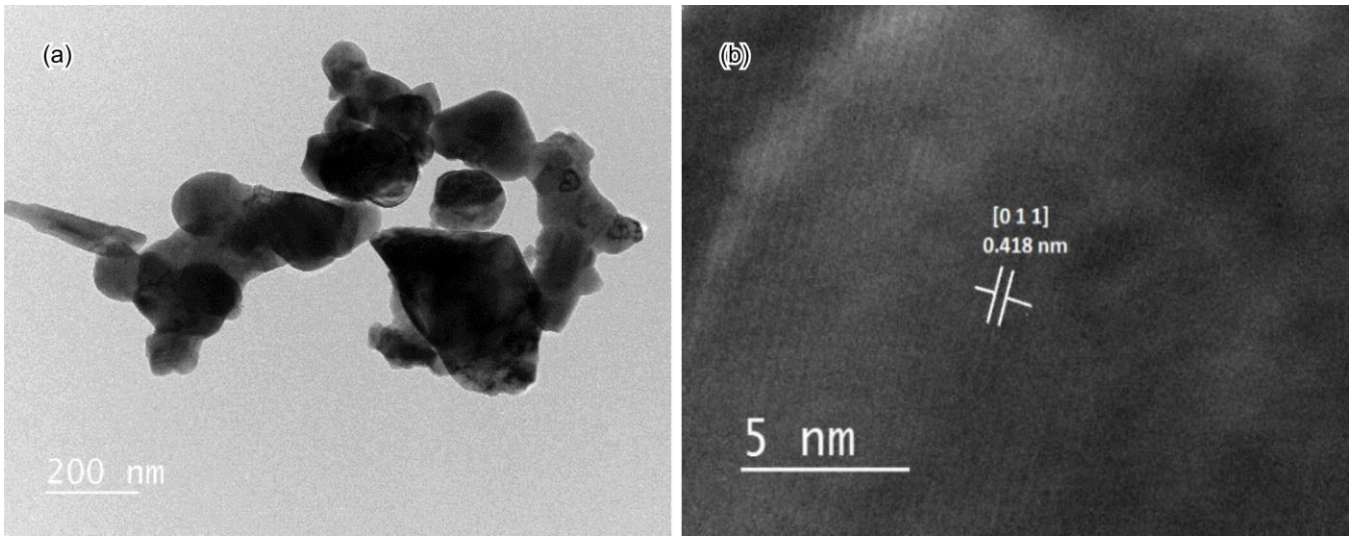

Fig. 3. (a) TEM and (b) HR-TEM of BT nanoparticles

(< 100 nm). It also confirmed that BT nanoparticles are in the crystalline in nature as shown in the HRTEM micrograph (Fig. 3b). The measured interplanar spacing is approximately 0.048 nm, which corresponds to the (011) crystallographic plane, as confirmed by the XRD spectra.

FTIR studies: FTIR is an effective tool for identifying the nature of chemical bonds and for confirming the formation of β-phase in PVDF polymers. The FTIR indicates the characteristic absorption peaks of PVDF polymer. The absorption peaks at 1401 cm^{-1} is for CH_2 bond. Two peaks at 1167 cm^{-1}

and 1070 cm^{-1} are corresponded to asymmetric and symmetric stretching vibration of CF_2. The absorption peaks at 610 cm^{-1} is for CF_2 bending and 876 cm^{-1} band is corresponded to C–H bending. The peaks around 839 and 781 cm^{-1} represents the asymmetric stretching vibrations of C–C–C and C–F bonds.

The FTIR spectra of PVDF, PVDF-BT and PVDF/GO/BT NP nanocomposite sheet is shown in Fig. 4. The absorption peaks at 840 cm^{-1}, 872 cm^{-1}, 1155 cm^{-1} and 1204 cm^{-1} indicate β-phase, whereas the peaks at 614 cm^{-1}, 763 cm^{-1} and 975 cm^{-1} affirm the α-phase. The bands at 790 cm^{-1} and 840 cm^{-1} show γ-phase. Bands at 1052 cm^{-1}, 840 cm^{-1}, 975 840 cm^{-1}, 838 cm^{-1} for C=C, C–O(alkoxy) correspond to groups of GO.

It is observed that the incorporation of nanofillers, namely BT nanoparticles and GO, into the PVDF matrix enhances the fraction of electroactive phases, specifically the β- and γ-phases. The fraction of β-phase formation can be calculated using eqn. 1, which is derived from the Beer-Lambert law. For this calculation, the absorption intensities of the characteristic peaks at 763 cm^{-1} and 836 cm^{-1} were considered.

$$F(\beta) = \frac{A_\beta}{1.26A_\alpha + A_\beta} \qquad (1)$$

where F(β) is the phase fraction of β-phase (electroactive), A_α and A_β are absorption intensities of 763 cm^{-1} and 836 cm^{-1}, respectively. The β-phase fraction of the pure PVDF film was approximately 40%. The incorporation of BT nanoparticles resulted in a slight improvement in β-phase content (~41%). In contrast, the addition of 0.1 wt.% GO significantly enhanced the β-phase fraction to about 50%, as also evidenced by the XRD patterns of the composite films. In addition to BT NPs, GO plays a crucial role in promoting the formation of electroactive phases in the PVDF polymer.

The composite film was further used to fabricate a nanogenerator (NG). The film was cut into dimensions of 20 mm (W) × 20 mm (L) × 1.0 mm (thickness), and a thin gold layer was deposited on both surfaces by sputtering. The film was then sandwiched between two aluminium electrodes and bonded using a commercially available epoxy resin with a premixed hardener, cured at room temperature, to enhance the mechanical robustness of the NG.

The energy-harvesting performance of the flexible NG was evaluated by applying a periodic dynamic load using a sewing machine operating at a fixed frequency, as illustrated in Fig. 5c. Under repeated mechanical excitation by the rod head, the NG generated an output voltage of approximately 11 V (peak-to-peak). The positive voltage originates from the transient flow of electrons under an external load, while the negative voltage observed in the absence of an external load is attributed to the reverse flow of charge carriers, resulting in the dissipation of the piezopotential (Fig. 5a). In addition, small voltage fluctuations were observed due to stack vibration and damping effects.

The NG produced a current of approximately 0.32 μA across a 1.5 MΩ load resistance, as shown in Fig. 5b. Furthermore, the energy-harvesting performance was investigated by varying the load resistance from 1 MΩ to 15 MΩ (Fig. 5b). The output power was calculated using eqn. 2 and the NG exhibited a maximum power output of approximately 3.3 μW under periodic mechanical tapping.

$$P = \frac{1}{t_2 - t_1}\int_{t_1}^{t_2} \frac{V^2}{R} dt \qquad (2)$$

where P is the power in mW; V is the real-time voltage; R is the load resistance; t_1 and t_2 are the initial and final time of output peak across the load resistance of R.

Conclusion

Lead free $BaTiO_3$ (BT) nanoparticles were synthesized using a hydrothermal process. PVDF/GO/BT nanocomposite films were fabricated by incorporating BT nanoparticles and graphene oxide (GO) as nanofillers into a PVDF matrix via a solution casting technique. The synthesized BT nanoparticles and the resulting nanocomposite films were characterized using various analytical techniques. The developed composite film was subsequently employed to fabricate a nanogenerator (NG) in a cost-effective and scalable manner. The performance of the nanogenerator was demonstrated under repeated mechanical tapping using a commercially available sewing machine. The NG exhibited a maximum output voltage of approximately 11 V and a power output of ~0.34 μW under mechanical exci-

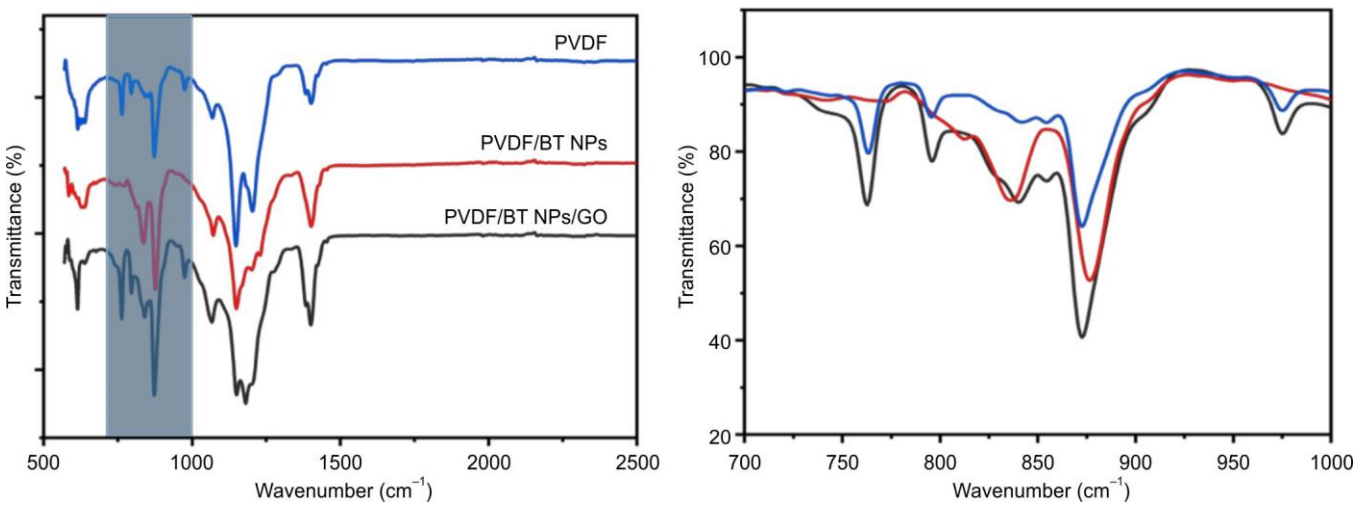

Fig. 4. FTIR spectra of PVDF and composite film

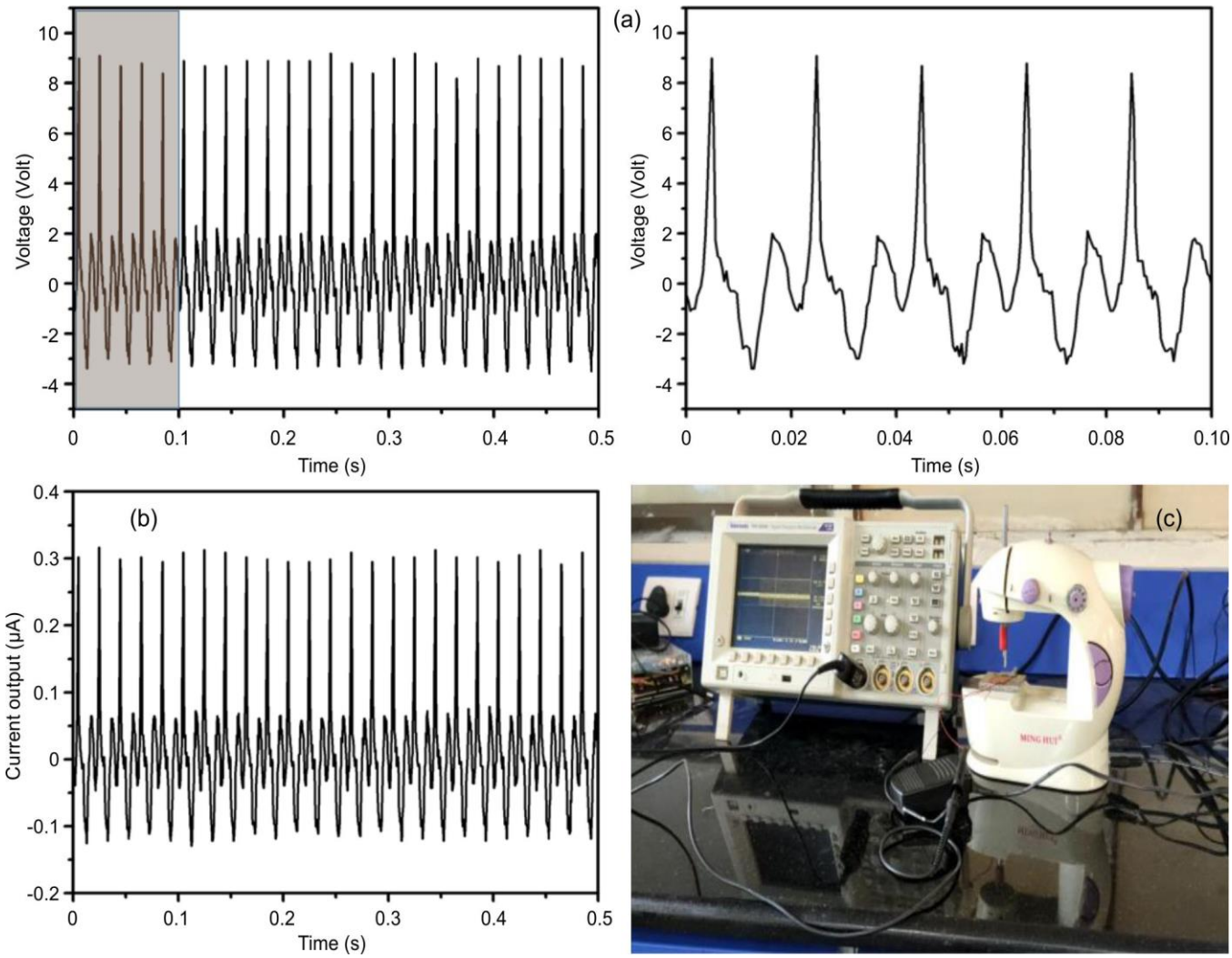

Fig. 5. (a) Measured voltage output exhibited by NG on mechanical repeated tapping, (b) Measured current output exhibited by NG across 1.5 MΩ on mechanical repeated tapping and (c) Test set for mechanical tapping on NG

tation. The robustness and durability of the fabricated NG were evaluated over 1000 cycles of continuous mechanical tapping.

ACKNOWLEDGEMENTS

The authors thank the Vice-Chancellor and Department of Chemistry, Mahatma Gandhi University, Nalgonda, for their support.

CONFLICT OF INTEREST

The authors declare that there is no conflict of interests regarding the publication of this article.

DECLARATION OF AI-ASSISTED TECHNOLOGIES

During the preparation of this manuscript, the authors used an AI-assisted tool(s) to improve the language. The authors reviewed and edited the content and take full responsibility for the published work.

REFERENCES

1. K.K. Jaiswal, C.R. Chowdhury, D. Yadav, R. Verma, S. Dutta, K.S. Jaiswal, B. Sangmesh and K.S.K. Karuppasamy, *Energy Nexus*, **7**, 100118 (2022); https://doi.org/10.1016/j.nexus.2022.100118
2. G.E. Halkos and E.-C. Gkampoura, *Energies*, **13**, 2906 (2020); https://doi.org/10.3390/en13112906
3. A.G. Olabi, K. Elsaid, K. Obaideen, M.A. Abdelkareem, H. Rezk, T. Wilberforce, H.M. Maghrabie and E.T. Sayed, *Int. J. Thermofluids*, **20**, 100498 (2023); https://doi.org/10.1016/j.ijft.2023.100498
4. T.-Z. Ang, M. Salem, M. Kamarol, H.S. Das, M.A. Nazari and N. Prabaharan, *Energy Strategy Rev.*, **43**, 100939 (2022); https://doi.org/10.1016/j.esr.2022.100939
5. A. Elkhatat and S. Al-Muhtaseb, *Energies*, **17**, 3179 (2024); https://doi.org/10.3390/en17133179
6. A.I. Osman, L. Chen, M. Yang, G. Msigwa, M. Farghali, S. Fawzy, D. W. Rooney and P.-S. Yap, *Environ. Chem. Lett.*, **21**, 741 (2023); https://doi.org/10.1007/s10311-022-01532-8
7. J. Briscoe and S. Dunn, *Nano Energy*, **14**, 15 (2015); https://doi.org/10.1016/j.nanoen.2014.11.059
8. S. Sapkal, B. Kandasubramanian and H.S. Panda, *J. Mater. Sci. Mater. Electron.*, **33**, 26633 (2022); https://doi.org/10.1007/s10854-022-09339-7

9. J. Ye, T. Xu and J.-C. Tan, *ACS Appl. Nano Mater.*, **8**, 3942 (2025); https://doi.org/10.1021/acsanm.4c06732
10. H. Ryu and S.W. Kim. *Small*, **17**, e1903469 (2021); https://doi.org/10.1002/smll.201903469
11. R. Ganeshkumar, C.W. Cheah, R. Xu, S.-G. Kim and R. Zhao, *Appl. Phys. Lett.*, **111**, 013905 (2017); https://doi.org/10.1063/1.4992786
12. S.-H. Shin, Y.-H. Kim, M.H. Lee, J.-Y. Jung and J. Nah, *ACS Nano*, **8**, 2766 (2014); https://doi.org/10.1021/nn406481k
13. B. Saravanakumar, S. Soyoon and S.-J. Kim, *ACS Appl. Mater. Interfaces*, **6**, 13716 (2014); https://doi.org/10.1021/am5031648
14. X. Pu, H. Guo, J. Chen, X. Wang, Y. Xi, C. Hu and Z.L. Wang, *Sci. Adv.*, **3**, e1700694 (2017); https://doi.org/10.1126/sciadv.1700694
15. C. Chang, V.H. Tran, J. Wang, Y.-K. Fuh and L. Lin, *Nano Lett.*, **10**, 726 (2010); https://doi.org/10.1021/nl9040719
16. B. Saravanakumar, R. Mohan, K. Thiyagarajan and S.-J. Kim, *RSC Advances*, **3**, 16646 (2013); https://doi.org/10.1039/c3ra40447a
17. Z.-H. Lin, Y. Yang, J.M. Wu, Y. Liu, F. Zhang and Z.L. Wang, *J. Phys. Chem. Lett.*, **3**, 3599 (2012); https://doi.org/10.1021/jz301805f
18. W. Wu, S. Bai, M. Yuan, Y. Qin, Z.L. Wang and T. Jing, *ACS Nano*, **6**, 6231 (2012); https://doi.org/10.1021/nn3016585
19. B. Rawal, P. Dixit, N.N. Wathore, B. Praveenkumar and H.S. Panda, *Bull. Mater. Sci.*, **43**, 82 (2020); https://doi.org/10.1007/s12034-020-2052-5
20. B. Rawal, P. Dixit, B. Praveenkumar and H.S. Panda, *J. Aust. Ceram. Soc.*, **55**, 729 (2019); https://doi.org/10.1007/s41779-018-0284-2
21. K.S. Chary, H.S. Panda and C.D. Prasad, *Ind. Eng. Chem. Res.*, **56**, 10335 (2017); https://doi.org/10.1021/acs.iecr.7b02182
22. H.M. Venkatesan, I. Woo, J.U. Yoon, P. Gajula, A.P. Arun and J.W. Bae, *Adv. Compos. Hybrid Mater.*, **8**, 221 (2025); https://doi.org/10.1007/s42114-025-01296-z
23. J.-C. Liou, C.-C. Diao, J.-J. Lin, Y.-L. Chen and C.-F. Yang, *Nanoscale Res. Lett.*, **9**, 1 (2014); https://doi.org/10.1186/1556-276X-9-1
24. K.S. Chary, V. Kumar, C.D. Prasad and H.S. Panda, *J. Aust. Ceram. Soc.*, **56**, 1107 (2020); https://doi.org/10.1007/s41779-020-00458-0
25. A. Teka, S. Bairagi, M. Shahadat, M. Joshi, S. Ziauddin Ahammad and S. Wazed Ali, *Polym. Adv. Technol.*, **29**, 2537 (2018); https://doi.org/10.1002/pat.4365